Atmos. Chem. Phys. Discuss., 14, 11075–11101, 2014
www.atmos-chem-phys-discuss.net/14/11075/2014/
doi:10.5194/acpd-14-11075-2014

Atmospheric Chemistry and Physics
Open Access
Discussions

Estimation of direct and indirect impacts of fireworks on the physicochemical characteristics of atmospheric fine and coarse particles

Y.-Z. Tian, J. Wang, X. Peng, G.-L. Shi, and Y.-C. Feng

State Environmental Protection Key Laboratory of Urban Ambient Air Particulate Matter Pollution Prevention and Control, College of Environmental Science and Engineering, Nankai University, Tianjin, 300071, China

Received: 26 February 2014 – Accepted: 22 April 2014 – Published: 6 May 2014

Correspondence to: G.-L. Shi (nksgl@hotmail.com)

Published by Copernicus Publications on behalf of the European Geosciences Union.

Abstract

To quantify total, direct and indirect impacts of fireworks individually, size-resolved PM samples were collected before, during, and after a Chinese folk-custom festival (Chinese New Year) in a megacity in China. Through chemical analysis and morphology characterization, strong influence of fireworks on physicochemical characteristics of PM_{10} and $PM_{2.5}$ was observed. Concentrations of many species exhibited an increasing trend during heavy-firework period, especially for K^+, Mg^{2+} and Cr; and the results of non-sea-salt ions demonstrated anthropogenic influence on them. Then, source apportionment was conducted by receptor models and Peak Analysis. Total influence of fireworks was quantified by PMF, showing that fireworks contributed rather higher fractions (23.40 % to PM_{10} and 29.66 % to $PM_{2.5}$) during heavy-firework period than those during light-firework period (4.28 % to PM_{10} and 7.18 % to $PM_{2.5}$). Profiles of total fireworks obtained by two independent methods (PMF and Peak Analysis) were consistent, with higher abundances of K^+, Al, Si, Ca and OC. Finally, individual contributions of direct and indirect impacts of fireworks were quantified by CMB. The percentage contributions of resuspended dust, biomass combustion and direct-fireworks were 36.82, 14.08 and 44.44 % for PM_{10} and 34.89, 16.60 and 52.54 % for $PM_{2.5}$, in terms of the total fireworks. The quantification of total, direct and indirect impacts of fireworks to ambient PM gives an original contribution to understand the physicochemical characteristics and mechanisms of such high-intensity anthropogenic activities.

1 Introduction

Atmospheric particulate matter (PM) is recognized as one of major environmental issues all over the world, with adverse effects on air quality, regional visibility, global climate change and health effects (Ding et al., 2008; Robichaud and Ménard, 2014). Through scattering and absorbing incoming solar radiation and outgoing terrestrial radiation directly, or acting as cloud condensation nuclei and thereby influencing the optical properties of clouds indirectly, atmospheric aerosols can influence the radiation balance of the earth atmosphere (Lin et al., 2013; Shen et al., 2013). Ambient PM is a complex mixture of components from a variety of sources, including natural and anthropogenic sources (Zheng et al., 2005; Zhao et al., 2013a). In recent years, concerns about short-term air quality degradation events and their continuous negative effects to human health has increased, especially for PM pollution caused by high-intensity anthropogenic activities.

Fireworks display is one of high-intensive anthropogenic activities that create notable air pollution and obvious short-term air quality degradation. Fireworks display is used to celebrate popular fiestas, a practice but common worldwide (e.g. at New Year). During firework episodes, there is usually a transient and spectacular increase of PM pollution. Fireworks contain a variety of metal salts such as chlorates and perchlorates, leading to extremely high ambient concentrations of these species during the celebration. These heavy metals and perchlorates are all high toxic (Shi et al., 2011), and are on average fine enough to be easily inhaled and show a health risk to susceptible individuals. Both long-term and short-term hazardous impacts of fireworks on human health have been paid significant attentions by the researchers (Wang et al., 2007; Vecchi et al., 2008; Crespo et al., 2012; Cheng et al., 2013).

Works demonstrated that displacement of fireworks could be an important source category to atmospheric PM (Vecchi et al., 2008). Fireworks could influence the PM directly, through emitting firework-related species (such as some heavy metals). What's more, the accessory effects, which were indirectly caused by activities of firework displays, should be taken into consideration in the firework events. For example, pyrotechnic device explosions would lead to resuspension of materials already deposited on the ground; and biomass combustion (firework is made by paper and cracker) occurs when the fireworks are displayed and incinerated after display. Although firework-related pollution episodes are transient in nature, they are highly concentrated and the influence is continuous. Both of direct and indirect influence of fireworks might significantly contribute to PM along with total annual metal emissions. However, the quantification of firework contributions, especially for its direct and indirect impacts, is very limited.

Studies on fireworks mainly applied the following methods: burning fireworks in specific laboratories or fields to characterize their chemical properties (Tsai et al., 2012); investigating environmental impacts through ambient sampling champion during firework periods (Sarkar et al., 2010; Crespo et al., 2012). The former couldn't reflect the actual ambient condition and indirect impacts. For the latter, celebrations by fireworks usually continued for only a few days. Thus, it was very difficult to quantify contributions of fireworks to ambient PM, especially for quantification of indirect impacts. Selecting an appropriate period and site for this subject is key. Firework is more prevalent in some places than others. China is the largest producing country of fireworks in the world (Shi et al., 2011). What's more, setting off fireworks is a traditional way to celebrate the Chinese New Year (CNY, Spring Festival) and justifiably welcomed all over the country. CNY is the most important and folk-custom holiday in China. Celebrations during CNY season tend to spill over to the preceding and succeeding days (usually till to Lantern Festival, another important festival in China), along with sporadic fireworks. During the firework episode, the anthropogenic emission patterns would be greatly changed (Huang et al., 2012). Many ordinary activities decreased, such as some industries and traffic (Feng et al., 2012); while degradation of air quality might occur due to display of fireworks. This provides a unique opportunity to study the drastic source changes and allows quantification of the direct and indirect contributions of fireworks under significantly different emission patterns.

Therefore, the purpose of this work is to individually quantify the total, direct and indirect contributions of fireworks to size-resolved PM. A sampling campaign of PM_{10} and $PM_{2.5}$ was carried out before, during, and after the CNY (as shown in Supplement Table S1) in a megacity in China. Physicochemical characteristics of PM during this folk-custom festival were investigated; the influence of fireworks on the physicochemical changes was also studied. The tracer species of fireworks were discussed and then used in the source identification. The total, direct and indirect contributions of fireworks to PM were modeled by Positive Matrix Factorization (PMF), Peak Analysis (PA) and Chemical Mass Balance (CMB) models. The quantitative assessment of fireworks' direct and indirect impacts to ambient PM gives an original contribution to understand the physicochemical characteristics and mechanisms during firework displays. The findings will aid in the studies on similar high-intensity anthropogenic activities.

2 Methodology

2.1 Sampling

The size-resolved PM samples were collected in Tianjin (a megacity in China). Tianjin, the largest harbor of Northern China, is a fast-growing and economically developed city who has a population of over 12 million and more than 1.5 million automobiles. The air quality of Tianjin declined with rapid urbanization and industrialization. The sampling site is sited at the rooftop of a six-story building which is located in a mixed residential and commercial area in Tianjin. Usually, substantial degradation would occur during the firework displays in such a mixed area. The map of the sampling site was indicated in Supplement Fig. S1.

The sampling campaign of PM_{10} and $PM_{2.5}$ was carried out from 30 January 2013 to 24 February 2013, including periods before, during, and after the CNY (till to Lantern Festival). The sampling periods and the corresponding Chinese Lunar calendar were listed in Supplement Table S1. During the sampling periods, firework displays took place for celebration of the CNY holiday. For the period from CNY's Eve to Lantern Festival, fireworks are allowed in China and numerous fireworks were consumed, thus, this period is defined as heavy-firework period. For the period before the CNY's Eve, sporadic fireworks might be set off, so light-firework period is defined.

Based on our previous works and other related studies (Shi et al., 2009; Xue et al., 2010; Harrison et al., 2012; Tian et al., 2013; Zhao et al., 2013a, b), the $PM_{2.5}$ and

PM_{10} were simultaneously collected on quartz fiber filters and polypropylene fiber filters using medium-volume air samplers (TH-150) at a flow rate of 100 L min^{-1}. The detailed information of sampling and quality assurance/quality control (QA/QC) were available in the Supplement.

2.2 Chemical analysis

The elemental compositions (Al, Si, Ca, V, Cr, Mn, Fe, Co, Cu, Zn, As and Pb) of the samples collected on polypropylene fiber filters were determined by inductively coupled plasma-mass spectrometry (ICP-AES) (IRIS Intrepid II, Thermo Electron). The ion chromatography (DX-120, DIONEX) was used to analyze the water soluble ions (NO_3^-, SO_4^{2-}, Na^+, K^+ and Mg^{2+}) collected on quartz fiber filters. Organic carbon (OC) and elemental carbon (EC) concentrations of the samples on quartz fiber filters were determined by means of DRI/OGC carbon analyzers, a technique based on the IMPROVE thermal/optical reflectance (TOR) protocol.

Background contamination was routinely monitored through blank tests. Enough blank tests were conducted and used to valid and correct corresponding data. Certified reference materials (CRM, produced by National Research Center for Certified Reference Materials, China) were used to ensure quality assurance and quality control. Blanks and duplicate sample analyses were carried out for nearly 10 % of samples. The pre-treatment procedure, chemical analysis and QA/QC are described in detail in the Supplement, referred to our previous works and other related studies (Bi et al., 2007; Shi et al., 2009; Wu et al., 2009; Kong et al., 2010; Xue et al., 2010; Zhao et al., 2013a, b).

In addition, scanning electron microscopy (SEM) determinations were performed by a JEOL JSM-7500F equipped with an X-ray energy dispersive spectrometer (EDS), to investigate morphology characterization and chemical analysis of individual particles.

2.3 Modeling approaches

2.3.1 Receptor models

Two widely-used receptor models, Positive Matrix Factorization (PMF) and Chemical Mass Balance (CMB), were applied to quantify the total (sum of direct and indirect contributions), direct and indirect contributions of fireworks.

PMF is a useful factorization methodology that can identify potential source categories and source contributions, when the source profiles are not known. It identifies the source profile matrix **F** and quantifies the source contribution matrix **G** based on observations at the receptor site (**X**). Following Paatro and Tapper (1994), PMF model can be represented in the matrix form as:

$$\mathbf{X} = \mathbf{G}\mathbf{F} + \mathbf{E} \tag{1}$$

The elements of source contribution matrix **G** and source profile matrix **F** are constrained to non-negative values for PMF. PMF uses the residual matrix elements (e_{ik}) and uncertainty estimates (σ_{ij}) to calculate a minimum Q value by using a weighed least square method, which is defined as:

$$Q(E) = \sum_{i=1}^{m} \sum_{j-1}^{n} (e_{ij}/\sigma_{ij})^2 \tag{2}$$

σ_{ij} is the uncertainty of the jth species in the ith sample, which is used to down weight the observations that include sampling errors, detection limits, missing data, and outliers (Paatero, 2007). The goal of PMF is to minimize this function.

PM data from different sizes ($PM_{2.5}$ and PM_{10}) were combined and inputted into PMF, as done in related works (Amato et al., 2009; Aldabe et al., 2011). The combined data showed the satisfactory results; and further analysis demonstrated that the profiles of $PM_{2.5}$ and PM_{10} were similar in this work. What's more, different numbers of factors and different Fpeak values were considered and tested when running PMF. Calculations were allowed to repeat ten times from ten pseudo-random starting points for each computation, to test if a global minimum point was reached. The error model code (EM = −14) and the uncertainties required for PMF were chosen according to the user's Guide (Paatero, 2007).

CMB is also a widely-used receptor model, when the number and profiles of sources are available (Watson et al., 1984; Chen et al., 2012). Similar with PMF, the CMB can be described as:

$$x_{ij} = \sum_{p=1}^{p} g_{ip} f_{pj} + e_{ij} \tag{3}$$

where x_{ij} is the jth species concentration measured in the ith sample; f_{pj} is the jth species mass fraction in the pth source; g_{ip} is the contribution of the pth source to the ith sample; and e_{ij} is the residual (Hopke, 2003). Different from PMF, except for x_{ij}, f_{pj} should also be available for CMB model. USEPA CMB8.2 (USEPA, 2004) was applied in this work. The main performance indices of CMB are reduced chi square (χ^2), percent mass (PM) and R square (R^2). Understanding the information of sources is important for the CMB modeling. In this work, field survey of sources was carried out before applying CMB model, to determine the source categories.

2.3.2 Peak Analysis

In the present study, Peak Analysis was used to quantify the species abundances of fireworks based on the observations of PM and chemical species. This method was successfully applied to determine profiles of vehicle emissions (Ke et al., 2013). The highest and lowest PM or species concentrations were used to represent peak and background observations, respectively. Peak period had the strongest fireworks density, while background values could be corresponded to the lowest fireworks density. Then, the species abundances were obtained by normalized their concentrations with corresponding PM concentrations, as follows (Ke et al., 2013):

$$F_j = \frac{c_{p,j} - c_{b,j}}{c_{p,\mathrm{PM}} - c_{b,\mathrm{PM}}} \tag{4}$$

where F_j is the abundance (g per g of PM) for the jth species, $C_{p,j}$ and $C_{b,j}$ are the jth species concentrations (µg m^{-3}) in the peak observation and the background observation, respectively; and $C_{p,\mathrm{PM}}$ and $C_{b,\mathrm{PM}}$ are the PM concentrations (µg m^{-3}) in the peak and the background observations, respectively.

The uncertainty (σ_{F_j}) of the jth species abundance (F_j) was defined as follows (Ke et al., 2013):

$$\sigma_{F_j} = F_j \sqrt{\left(\frac{\sigma_{p,j}}{c_{p,j}}\right)^2 + \left(\frac{\sigma_{b,j}}{c_{b,j}}\right)^2} \tag{5}$$

where $\sigma_{p,j}$ and $\sigma_{b,j}$ are the measurement uncertainties (µg m^{-3}) of the jth species in the peak observation and the background observation, respectively. The results of Peak Analysis method were employed to describe profiles of the total fireworks.

3 Results and discussion

3.1 Physicochemical characteristics of PM$_{10}$ and PM$_{2.5}$

PM samples were acquired on two filters for each sampling day, so consistency tests play an important role in QA/QC process. The comparisons between concentrations measured on polypropylene fiber filters and those on quartz fibre filters were shown in Supplement Fig. S2. Satisfactory consistency (slopes close to unit and high correlations) were observed, indicating good quality assurance. Due to the reason that quartz fibre filters tend to absorb water and be shredded during sampling handling (Cheng et al., 2011), concentrations on polypropylene fiber filters were used in the following discussion.

The concentrations of the PM_{10} and $PM_{2.5}$ in Tianjin during sampling periods are summarized in Supplement Fig. S3. The averaged concentration of PM_{10} was 212.95 $\mu g\,m^{-3}$ and that of $PM_{2.5}$ was 140.59 $\mu g\,m^{-3}$, with an averaged ratio of $PM_{2.5}/PM_{10}$ being 0.66. The PM_{10} and $PM_{2.5}$ concentrations were 148.74 and 96.80 $\mu g\,m^{-3}$ during light-firework period and 249.08 and 165.23 $\mu g\,m^{-3}$ during heavy-firework period. The highest concentrations were observed at CNY's Eve when massive firework displays usually take place all over the country (Feng et al., 2012), indicating the huge influence of fireworks on PM concentrations.

Study on chemical composition is critical for understanding the physicochemical characteristics of pollution during the folk-custom festival. The averaged concentrations of the chemical species in PM_{10} and $PM_{2.5}$ during the light-firework period and the heavy-firework period were exhibited in Fig. 1; and the abundances of species (fractions of species in PM) in PM_{10} and $PM_{2.5}$ were summarized in Supplement Table S2. According to Fig. 1 and Table S2 in the Supplement, crustal elements (Al, Si, Fe, Ca), carbonaceous species (OC and EC), some water-soluble ions (Cl^-, NO_3^- and SO_4^{2-}) were important species in PM_{10} and $PM_{2.5}$ during sampling periods. What's more, it is interesting to find that K^+ also played an important role during heavy-firework period, which was much lower during light-firework period.

In addition, for a further characterization, the quartz fibre filters photos and micrographs were exhibited. In Fig. S4 of the Supplement, photos of quartz filters of PM_{10} and $PM_{2.5}$ samples were in two cases: a common day in the light-firework period and the CNY's Eve in the heavy-firework period. Difference between filters can be observed. Furthermore, micrographs of $PM_{2.5}$ for the fore-mentioned days were shown in Supplement Fig. S5. There were much more particles for samples of the CNY's Eve than those of the common day, demonstrating the much higher concentration levels in the CNY's Eve.

3.2 Influence of fireworks on physicochemical characteristics of PM pollution

Comparing the mass concentrations and abundances of species during heavy-firework period with those during light-firework period would help researchers learn more on the influence of this intensive human activity. As shown in Fig. 1, concentrations of most species (like crustal elements, heavy mental species, carbonaceous specie, Cl^-, Na^+, K^+, and Mg^{2+}) exhibited an increasing trend during heavy-firework period. Al, Ca, Cr, Cu, Pb, Cl^-, Na^+, K^+, and Mg^{2+} might represent the firework-related species. Potassium is one of the major components of fireworks, because potassium compounds in black powder (commonly in the form perchlorate or chlorate) act as the main oxidizer during burning, with the corresponding chemical equations being $2KClO_3 = 2KCl + 3O_2$ and $KClO_4 = KCl + 2O_2$. Ca compounds (such as the chloride and sulphate) and Cu compounds (such as the chloride and oxide) give rise to orange and blue colourations, respectively. Cr compounds ($CuCr_2O_4$) is used as a catalyst for propellents. Cu, K, and Cr are used to provide silvery and glitter effects as well. Mg is a useful metallic fuel and is also used to produce sparks and crackling stars (in the form of a 50 : 50 Mg : Al alloy magnalium). Al also could be used alone as a common constituent for fuel, sparks and glitter effects. Pb could help to achieve steady and reproducible burning rates. Many components are in the form of perchlorate or chlorate, leading to high concentrations of Cl^-. The abruptly high emissions of these elements due to firework burning activities can explain high concentrations of these firework-related species in atmospheric PM during heavy-firework period. It's worthy to be noted that some firework-related heavy metals (Cr, Pb Cu etc.) are dangerous elements because of their toxicity, and are forbidden by laws in many countries. Such very high concentrations in a short time, especially in a place where considerable people are gathered, might be of concern.

Except for the direct firework-related species, an increase was also observed for most of the crustal elements (such as Al, Si and Ca). Although Al and Ca might from industrial and direct firework sources, abrupt increase of crustal elements might also due to the resuspension of materials already deposited on the ground, caused by pyrotechnic device explosions. Additionally, higher concentration of K^+ and also of OC, which are good markers of biomass combustion, might imply the contribution of biomass combustion during the heavy-firework period. The higher concentrations of those indirect-related markers during the heavy-firework period can be ascribed partly to indirect influence of fireworks. Such important contributions of the resuspended dust and the biomass combustion must be taken into consideration as sources of PM in these firework events. Moreover, the mass ratios of the NO_3^- to SO_4^{2-} (NO_3^-/SO_4^{2-}) during heavy-firework period were lower than ratios during light-firework period. Similarly, lower NO_3^-/SO_4^{2-} during CNY was observed in Beijing (Feng et al., 2012). The change of NO_3^-/SO_4^{2-} might be partly due to their different formation mechanism. Wang et al. (2007) reported the dominance of metal-catalyzed heterogeneous formation of sulfate during the firework period. Goodman et al. (2001) reported the different formation mechanism of nitrate. However, the formation of secondary particles might be influenced by considerable factors (like meteorological conditions and precursors) and is very complex.

Some of fore-mentioned species need a further study. SEM micrographs and EDS spectra of particles in the common day and in the CNY's Eve were exhibited in Supplement Fig. S6. The Individual particle analysis showed the rater higher K in the CNY's Eve than in the common day. Furthermore, the species that particularly stand out as present in concentrations during heavy-firework period far higher than those during light-firework period are K^+, Cr, and Mg^{2+}. The H/L values (the ratios of concentrations in heavy-firework period to those in light-firework period) of K^+, Cr, and Mg^{2+} concentrations were 6.29, 5.52, 3.97 for PM_{10} and 5.78, 4.63, 6.32 for $PM_{2.5}$ (as shown in Fig. 1). The mass concentrations might not completely reflect the composition of PM, so the comparison between species abundances was also conducted. As shown in Supplement Table S2, the abundances of K^+, Cr, and Mg^{2+} were obviously higher during heavy-firework period, with H/L of 3.08, 4.44, 1.78 for PM_{10} and 2.68, 2.06 and 2.37 for $PM_{2.5}$. The high H/L of abundances can demonstrate the intensive influence of fireworks on these species. For a further investigation, the daily variations of concentrations and abundances of the most firework-influenced species (K^+, Mg^{2+} and Cr) were shown in Supplement Fig. S7. Similar time patterns were observed for these species. Both of the mass concentrations and abundances of K^+, Mg^{2+} and Cr showed sharp peaks at CNY's Eve, in $PM_{2.5}$ and PM_{10}. Obvious increases also occurred at the fifth day of Chinese Lunar calendar and Lantern Festival, which were important folk-custom days for fireworks. Thus, K^+, Mg^{2+} and Cr could indicate the fireworks influence, which is important for further identification of fireworks source category.

Species in PM might come from anthropogenic and natural sources. To focus the characteristics of anthropogenic emissions, the non-sea-salt (nss) ions were computed. Assuming that all of the Na^+ were from sea salt, the concentrations of nss-SO_4^{2-}, nss-Cl^-, nss-K^+ and nss-Mg^{2+} in PM_{10} and $PM_{2.5}$ were calculated based on the composition of average sea water. Relative mass concentrations of SO_4^{2-}, Cl^-, K^+ and Mg^{2+} to Na^+ are 0.252, 1.8, 0.037 and 0.119 (Feng et al., 2012). Nearly all SO_4^{2-} and K^+ (> 98 %), most Mg^{2+} (> 75 %) in both PM_{10} and $PM_{2.5}$ are from non-sea-salt. It's interesting to find higher percentage of nss-Cl^-in $PM_{2.5}$ (72 %) than in PM_{10} (57 %), indicating stronger influence of anthropogenic emissions on Cl^- in fine PM. This result is reasonable because sea salt contributes higher fraction to coarse fraction of PM (Keuken et al., 2013). To investigate the anthropogenic impacts of fireworks, a comparison was conducted between nss-ions during light-firework and heavy-firework periods. There was no obvious difference for nss-SO_4^{2-}. The concentrations of nss-Cl^-, nss-K^+ and nss-Mg^{2+} as well as their percentage in total ions were exhibited in Supplement Fig. S8. For these three ions, much higher concentrations and higher percentages occurred during heavy-firework period, especially at CNY's Eve with above 88 % ions from anthropogenic impacts. These results suggest the large anthropogenic influence on Cl^-, K^+, Mg^{2+} which might be mainly caused by fireworks during the Chinese folk-custom festival; and they were effective to indicate the fireworks. In the present work, the sources to Cl^- are complex, including not only anthropogenic but also natural sources (Vassura et al., 2014). Additionally, considering too lower concentrations of Cr in the PM mass, K^+ and Mg^{2+} might be more powerful to be the tracers of fireworks in the following source apportionment, similar with related literatures (Wang et al., 2007; Cheng et al., 2013).

3.3 Sources of PM

To quantitatively evaluate the total, direct and indirect impacts of fireworks on ambient PM, source apportionment of size-resolved PM samples were modeled by PMF, Peak Analysis and CMB models in this section.

3.3.1 Total contributions of fireworks by PMF modeling

PMF was firstly applied to identify the possible source categories and to quantify their contributions to PM during sampling periods. Through checking the variation in Q values and model performance, five factors solution and $F\text{peak} = 0.1$ were determined for fitting. The fitting plot between the measured and estimated PM concentrations was exhibited in Supplement Fig. S9. The slope of regression was 0.96 and the Pearson correlation coefficient was 0.98, suggesting perfect performance of PMF in this run (the estimated PM concentrations for most samples were close to the measured concentrations).

The source profiles obtained by PMF are listed in Fig. 2. According to Fig. 2, Factor 1 exhibited high loading for Al, Si, Ca etc., which are associated with crustal dust (Pant and Harrison et al., 2012). In Factor 2, relatively higher loadings of Al, Si and OC were observed. Previous studies demonstrated that high Al, Si and OC at the same time might indicate the source category of coal combustion (Zhang et al., 2011; Pant and Harrison et al., 2012). Factor 3 correlates strongly with SO_4^{2-} and NO_3^-, consistent with source categories related to secondary particles (secondary sulphate and secondary nitrate) (Gao et al., 2011; Tian et al., 2013). Factor 4 is mainly characterized by OC and EC, which were indicatives of vehicular exhaust (Pant and Harrison et al., 2012).

The percentage contributions of these source categories were summarized in Fig. 2 as well.

In Factor 5, K^+ presented obviously high weightings. As discussed above, K^+ might be the tracer of fireworks, and higher loading of Mg^{2+} in this factor might also indicate the impacts of fireworks. Furthermore, it's interesting to find relatively higher weightings of other species, like OC, Al, Si and Ca. Strong links with K^+ and OC could demonstrate the biomass combustion (Cheng et al., 2013). Factor 5 was also associated with Al, Si and Ca which are crustal elements. Biomass combustion might be indirectly caused by fireworks, which might occur when the fireworks are displayed and incinerated after display. Crustal elements might from the resuspension of materials already deposited on the ground (caused by pyrotechnic device explosions). Therefore, Factor 5 was the total influence of fireworks, which might include direct-fireworks contribution and indirect impacts (biomass combustion and resuspended dust). PMF extracts source profiles and quantifies contributions based on the temporal variation of chemical species, so source categories in one emission pattern might be identified as one factor. In this work, direct-fireworks, resuspended dust and biomass combustion caused by fireworks might have the similar emission pattern.

As exhibited in Fig. 2, the total influence of fireworks, including direct-fireworks and indirect impacts, contributed 19.29 % to PM_{10} and 24.09 % to $PM_{2.5}$ during the whole sampling periods. The averaged percentage source contributions to PM_{10} and $PM_{2.5}$ during the light-firework and heavy-firework periods are respectively calculated and shown in Fig. 3. Much difference can be observed. During the light-firework period, the total influence of fireworks contributed 4.28 % to PM_{10} and 7.18 % to $PM_{2.5}$; while during the heavy-firework period, the total influence of fireworks enhanced to rather high fractions (23.40 % to o PM_{10} and 29.66 % to $PM_{2.5}$). The time series of percentage contributions of total firework impacts to PM_{10} and $PM_{2.5}$ were exhibited in Fig. 4, which could present the trend of total firework impacts (including direct-fireworks, resuspended dust and biomass combustion). The most significant peak of total firework contributions was presented in the CNY's Eve, indicating the heavy impacts of total fireworks in this day, although the contributions might be overestimated due to the uncertainties of results by PMF. In most cities in China, firework is allowed from CNY's Eve to Lantern Festival (namely the heavy-firework period in this work). Numerous fireworks were displayed in the night of CNY's Eve, as it's the most important celebration in one year. Another peak of firework contributions was observed in Lantern Festival. Lantern Festival is also an important festival in China and is the last day for allowance of fireworks. The variation of firework contributions consisted with the Chinese folks for celebration, which could demonstrate the good performance of PMF for modeling total firework contributions in this work.

3.3.2 Species abundances of total firework impacts

Except for PMF, Peak Analysis was also employed for a better understanding of total firework impacts. As discussed above, profiles and contributions of total firework impacts were determined by PMF for PM_{10} and $PM_{2.5}$. Furthermore, Peak Analysis (Ke et al., 2013) was employed in this section to investigate the species abundances of total fireworks in terms of the observations. The species abundances of total firework impacts obtained by the two independent methods (PMF and Peak Analysis) were exhibited in Fig. 5. Considering the complexity as fore-mentioned, the secondary ions weren't included in the comparison. Comparing the firework profiles, the abundances of most chemical species by Peak Analysis were similar to the corresponding values by PMF. As shown in Fig. 5, the abundance of K^+, which is the main marker of direct-fireworks as discussed above, were harmonious in three firework profiles, with values of 16.34 % by PMF, 15.21 % by Peak Analysis for PM_{10} and 17.33 % by Peak Analysis for $PM_{2.5}$. Al, Si and Ca (resuspended dust elements) as well as OC (marker of biomass combustion along with K^+) were also in agreement. The abundances of Al were 5.87, 6.72 and 7.02 %; Si were 9.87, 10.07 and 11.85 %; OC were 6.32, 5.87 and 6.60 %, estimated by PMF, by Peak Analysis for PM_{10} and by Peak Analysis for $PM_{2.5}$, respectively. For a further investigation of the similarity among these profiles, regression analysis and correlation coefficients (R) were computed and shown in Fig. 5. It is visible from Fig. 5 that all correlation coefficients were higher than 0.9, suggesting that total firework profiles obtained by PMF and by Peak Analysis were concordant. In addition, firework profiles of $PM_{2.5}$ were similar with that of PM_{10}, implying the reasonability to introduce the combined dataset of $PM_{2.5}$ and PM_{10} into PMF.

3.3.3 Contributions of direct and indirect firework impacts

As discussed above, the total influence of fireworks might include indirect impacts (resuspended dust, biomass combustion) and direct-fireworks. Thus, it is necessary to deeply evaluate the individual impacts of fireworks. In this work, the total firework profiles calculated by Peak Analysis were applied as the receptors in the CMB model, and source profiles of three contributors (resuspended dust, biomass combustion and direct-firework) were incorporated into the model, to individually determine direct and indirect impacts of fireworks. In this work, the source profiles of resuspended dust were from our prior works in Tianjin (Zhang et al., 2011); biomass combustion profiles were from speciate 4.0 of US EPA; firework profiles were referred to a reported work (Tsai et al., 2012). The performance indices of CMB in this work were summarized in Supplement Table S3. The values of the performance indices met the requirement, indicating that results of CMB might be reliable.

The individual contributions to the total firework impacts (based on Peak Analysis) were exhibited in Fig. 3. According to the estimations, the percentage contributions of resuspended dust, biomass combustion and direct-fireworks were 36.82, 14.08 and 44.44 % for PM_{10}, accounting for the total fireworks contribution. For $PM_{2.5}$, the percentage contributions were estimated to be 34.89 % from resuspended dust, 16.60 % from biomass combustion, and 52.54 % from direct-fireworks. The results demonstrated that fireworks could lead to comprehensive influence to the ambient PM. Except for the direct-fireworks influence, resuspended dust and biomass combustion caused by fireworks indirectly should also be paid attention to.

4 Conclusions

To quantify total, direct and indirect impacts of fireworks, size-resolved PM samples were collected in a megacity in China. The sampling campaign covered a Chinese folk-custom festival (CNY), which provides a unique opportunity to quantify contributions of fireworks under significantly different emission patterns. Strong influence of fireworks on physicochemical characteristics of atmospheric fine and course particles was observed. The highest PM concentrations were observed at CNY's Eve when massive firework displays usually take place all over the country. Concentrations of most species (like crustal elements, heavy mental species, carbonaceous specie, Cl^-, Na^+, K^+, and Mg^{2+}) exhibited an increased trend during heavy-firework period. Among them, K^+, Mg^{2+} and Cr showed the most obvious increase; and the results of non-sea-salt ions demonstrated the anthropogenic influence on these species. K^+, Mg^{2+} and Cr could be good tracers of fireworks, especially for K^+ and Mg^{2+} who had higher concentrations. Then, source apportionment was conducted by receptor models. Total influence of fireworks was quantified by PMF, contributing rather higher fractions during heavy-firework period than those during light-firework period. Profiles of total fireworks obtained by PMF and Peak Analysis were consistent, with higher abundances of K^+, Al, Si, Ca and OC. Finally, individual contributions of direct and indirect impacts of fireworks were determined by CMB model based on profiles from Peak Analysis. The present study demonstrated that fireworks might lead to comprehensive influence to the ambient PM. Both of the direct influence and indirect impacts (resuspended dust and biomass combustion) caused by fireworks should be paid attention to. The present work would be helpful for understanding the physicochemical characteristics and mechanisms of such high-intensity anthropogenic activities.

Supplementary material related to this article is available online at http://www.atmos-chem-phys-discuss.net/14/11075/2014/acpd-14-11075-2014-supplement.pdf.

Acknowledgements. This study is supported by the National Natural Science Foundation of China (21207070 and 41375132), Special Funds for Research on Public Welfares of the Ministry of Environmental Protection of China (201409003) and the Combined Laboratory of the Tianjin Meteorological Bureau.

References

Aldabe, J., Elustondo, D., Santamaría, C., Lasheras, E., Pandolfi, M., Alastuey, A., Querol, X., and Santamaría, J. M.: Chemical characterisation and source apportionment of $PM_{2.5}$ and PM_{10} at rural, urban and traffic sites in Navarra (North of Spain), Atmos. Res., 1, 191–205, 2011.

Amato, F., Pandolfi, M., Escrig, A., Querol, X., Alastuey, A., Pey, J., Perez, N., and Hopke, P. K.: Quantifying road dust resuspension in urban environment by multilinear engine: a comparison with PMF2, Atmos. Environ., 17, 2770–2780, 2009.

Bi, X. H., Feng, Y. C., Wu, J. H., Wang, Y. Q., and Zhu, T.: Source apportionment of PM_{10} in six cities of northern China, Atmos. Environ., 41, 903–912, 2007.

Chen, L.-W. A., Watson, J. G., Chow, J. C., Green, M. C., Inouye, D., and Dick, K.: Wintertime particulate pollution episodes in an urban valley of the Western US: a case study, Atmos. Chem. Phys., 12, 10051–10064, doi:10.5194/acp-12-10051-2012, 2012.

Cheng, Y., Zou, S. C., Lee, S. C., Chow, J. C., Ho, K. F., Watson, J. G., Han, Y. M., Zhang, R. J., Zhang, F., Yau, P. S., Huang, Y., Bai, Y., and Wu, W. J.: Characteristics and source apportionment of PM_1 emissions at a roadside station, J. Hazard. Mater., 195, 82–91, 2011.

Cheng, Y., Engling, G., He, K.-B., Duan, F.-K., Ma, Y.-L., Du, Z.-Y., Liu, J.-M., Zheng, M., and Weber, R. J.: Biomass burning contribution to Beijing aerosol, Atmos. Chem. Phys., 13, 7765–7781, doi:10.5194/acp-13-7765-2013, 2013.

Crespo, J., Yubero, E., Nicolás, J. F., Lucarelli, F., Nava, S., Chiari, M., Calzolai, G.: High-time resolution and size-segregated elemental composition in high-intensity pyrotechnic exposures, J. Hazard. Mater., 241, 82–91, 2012.

Ding, X., Zheng, M., Yu, L. P., Zhang, X. L., Weber, R. J., Yan, B., Russell, A. G., Edgerton, E. S., and Wang, X. M.: Spatial and seasonal trends in biogenic secondary organic aerosol tracers and water-soluble organic carbon in the southeastern United States, Environ. Sci. Technol., 42, 5171–5176, 2008.

Feng, J. L., Sun, P., Hu, X. L., Zhao, W., Wu, M. H., and Fu, J. M.: The chemical composition and sources of PM$_{2.5}$ during the 2009 Chinese New Year's holiday in Shanghai, Atmos. Res., 118, 435–444, 2012.

Gao, X., Yang, L., Cheng, S., Gao, R., Zhou, Y., and Xue, L.: Semi-continuous measurement of water-soluble ions in PM$_{2.5}$ in Jinan, China: temporal variations and source apportionments, Atmos. Environ., 45, 6048–6056, 2011.

Goodman, A. L., Bernard, E. T., and Grassian, V. H.: Spectro-scopic study of nitric acid and water adsorption on oxide particles: enhanced nitric acid uptake kinetics in the presence of adsorbed water, J. Phys. Chem. A, 105, 6443–6457, 2001.

Hopke, P. K.: Recent developments in receptor modeling, J. Chemometr., 17, 255–265, 2003.

Huang, K., Zhuang, G., Lin, Y., Wang, Q., Fu, J. S., Zhang, R., Li, J., Deng, C., and Fu, Q.: Impact of anthropogenic emission on air quality over a megacity – revealed from an intensive atmospheric campaign during the Chinese Spring Festival, Atmos. Chem. Phys., 12, 11631–11645, doi:10.5194/acp-12-11631-2012, 2012.

Ke, H. H., Ondov, J. M., and Rogge, W. F.: Detailed emission profiles for on-road vehicles derived from ambient measurements during a windless traffic episode in Baltimore using a multi-model approach, Atmos. Environ., 81, 280–287, 2013.

Keuken, M. P., Moerman, M., Voogt, M., Blom, M., Weijers, E. P., Röckmann, T., and Dusek, U.: Source contributions to PM$_{2.5}$ and PM$_{10}$ at an urban background and a street location, Atmos. Environ., 71, 26–35, 2013.

Kong, S. F., Han, B., Bai, Z. P., Chen, L. Shi, J. W., and Xu, J. W.: Receptor modeling of PM$_{2.5}$, PM$_{10}$ and TSP in different seasons and long-range transport analysis at a coastal site of Tianjin, China, Sci. Total Environ., 408, 4681–4694, 2010.

Lin, Z. J., Tao, J., Chai, F. H., Fan, S. J., Yue, J. H., Zhu, L. H., Ho, K. F., and Zhang, R. J.: Impact of relative humidity and particles number size distribution on aerosol light extinction in the urban area of Guangzhou, Atmos. Chem. Phys., 13, 1115–1128, doi:10.5194/acp-13-1115-2013, 2013.

Paatero, P.: User's Guide for Positive Matrix Factorization Programs PMF2 and PMF3, Part 1–2: Tutorial, University of Helsinki, Helsinki, Finland, 2007.

Paatero, P., Tapper, U.: Positive Matrix Factorization: a non-negative factor model with optimal utilization of error estimates of data values, Environmetrics, 5, 111–126, 1994.

Pant, P. and Harrison, R. M.: Critical review of receptor modelling for particulate matter: a case study of India, Atmos. Environ., 49, 1–12, 2012.

Robichaud, A. and Ménard, R.: Multi-year objective analyses of warm season ground-level ozone and $PM_{2.5}$ over North America using real-time observations and Canadian operational air quality models, Atmos. Chem. Phys., 14, 1769–1800, doi:10.5194/acp-14-1769-2014, 2014.

Sarkar, S., Khillare, P. S., Jyethi, D. S., Hasan, A., Parween, M.: Chemical speciation of respirable suspended particulate matter during a major firework festival in India, J. Hazard. Mater., 184, 321–330, 2010.

Shen, G. F., Tao, S., Wei, S. Y., Chen, Y. C., Zhang, Y. Y., Shen, H. Z., Huang, Y., Zhu, D., Yuan, C. Y., Wang, H. C., Wang, Y. F., Pei, L. J., Liao, Y. L., Duan, Y. H., Wang, B., Wang, R., Lv, Y., Li, W., Wang, X. L., and Zheng, X. Y.: Field measurement of emission factors of PM, EC, OC, parent, nitro, and oxy-polycyclic aromatic hydrocarbons for residential briquette, coal cake, and wood in rural Shanxi, China, Environ. Sci. Technol., 47, 2998–3005, 2013.

Shi, G. L., Feng, Y. C., Zeng, F., Li, X., Zhang, Y. F., and Wang, Y. Q.: Use of a nonnegative constrained principal component regression chemical mass balance model to study the contributions of nearly collinear sources, Environ. Sci. Technol., 43, 8867–8873, 2009.

Shi, Y. L., Zhang, N., Gao, J. M., Li, X., Cai, Y. Q.: Effect of fireworks display on perchlorate in air aerosols during the Spring Festival, Atmos. Environ., 45, 1323–1327, 2011.

Tian, Y. Z., Shi, G. L., Han, S. Q., Zhang, Y. F., Feng, Y. C., Liu, G. R., Gao, L. J., Wu, J, H., and Zhu, T.: Vertical characteristics of levels and potential sources of water-soluble ions in PM_{10} in a Chinese megacity, Sci. Total Environ., 447, 1–9, 2013.

Tsai, H. H., Chien, L. H., Yuan, C. S., Lin, Y. C., Jen, Y. H., and Ie, I. R.: Influences of fireworks on chemical characteristics of atmospheric fine and coarse particles during Taiwan's Lantern Festival, Atmos. Environ., 62, 256–264, 2012.

US Environmental Protection Agency: EPA-CMB8.2 Users Manual, US EPA, Office of Air Quality Planning and Standards, Research Triangle Park, NC 27711, 2004.

Vassura, I., Venturini, E., Marchetti, S., Piazzalunga, A., Bernardi, E., Fermo, P., and Passarini, F.: Markers and infiuence of open biomass burning on atmospheric particulate size and composition during a major bonfire event, Atmos. Environ., 82, 21–225, 2014.

Vecchi, R., Bernardoni, V., Cricchio, D., D'Alessandro, A., Fermo, P., Lucarelli, F., Nava, S., Piazzalunga, A., and Valli, G.: The impact of fireworks on airborne particles, Atmos. Environ., 42, 1121–1132, 2008.

Wang, Y., Zhuang, G. S., Xu, C., and An, Z. S.: The air pollution caused by the burning of fireworks during the lantern festival in Beijing, Atmos. Environ., 41, 417–431, 2007.

Watson, J. G., Cooper, J. A., and Huntzicker, J. J.: The effective variance weighting for least squares calculations applied to the mass balance receptor model, Atmos. Environ., 18, 1347–1355, 1984.

Wu, L., Feng, Y. C., Wu, J. H., Zhu, T., Bi, X. H., Han, B., Yang, W. H., and Yang, Z. Q.: Secondary organic carbon quantification and source apportionment of PM_{10} in Kaifeng, China, J. Environ. Sci., 21, 1353–1362, 2009.

Xue, Y. H., Wu, J. H., Feng, Y. C., Dai, L., Bi, X. H., and Li, X.: Source characterization and apportionment of PM_{10} in Panzhihua, China, Aerosol Air Qual. Res., 10, 367–377, 2010.

Zhang, Y. F., Xu, H., Tian, Y. Z., Shi, G. L., Zeng, F., Wu, J. H., Zhang, X. Y., Li, X., Zhu, T., and Feng, Y. C.: The study on vertical variability of PM_{10} and the possible sources on a 220 m tower, in Tianjin, China, Atmos. Environ., 45, 6133–6140, 2011.

Zhao, P. S., Dong, F., He, D., Zhao, X. J., Zhang, X. L., Zhang, W. Z., Yao, Q., and Liu, H. Y.: Characteristics of concentrations and chemical compositions for $PM_{2.5}$ in the region of Beijing, Tianjin, and Hebei, China, Atmos. Chem. Phys., 13, 4631–4644, doi:10.5194/acp-13-4631-2013, 2013.

Zhao, X. J., Zhao, P. S., Xu, J., Meng„ W., Pu, W. W., Dong, F., He, D., and Shi, Q. F.: Analysis of a winter regional haze event and its formation mechanism in the North China Plain, Atmos. Chem. Phys., 13, 5685–5696, doi:10.5194/acp-13-5685-2013, 2013.

Zheng, M., Salmon, L. G., Schauer, J. J., Zeng, L. M., Kiang, C. S., Zhang, Y. H., and Cass, G. R.: Seasonal trends in $PM_{2.5}$ source contributions in Beijing, China, Atmos. Environ., 39, 3967–3976, 2005.

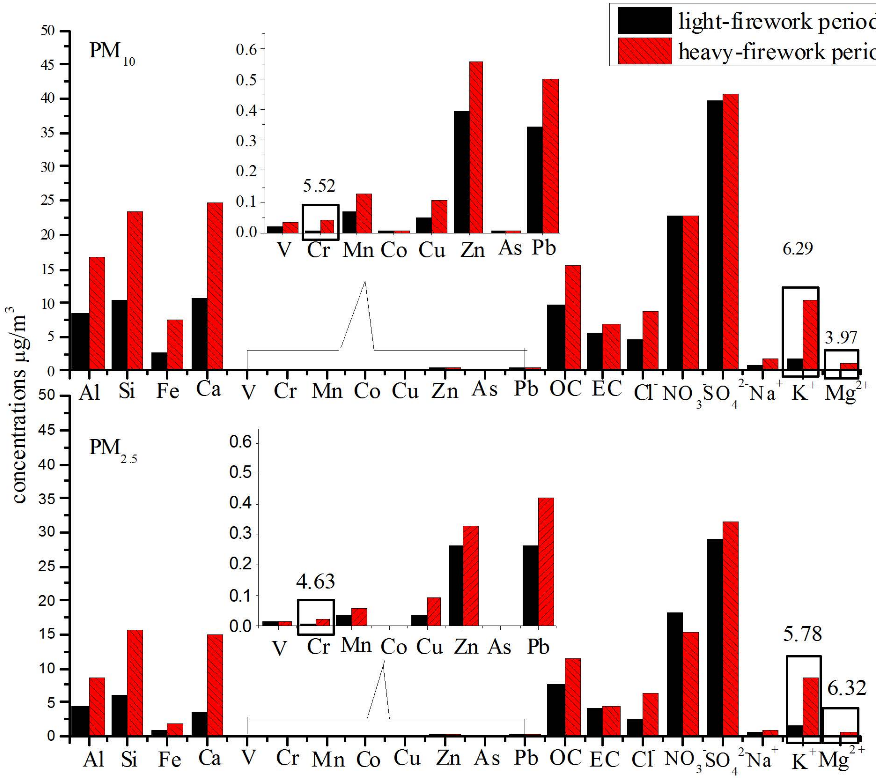

Fig. 1. The averaged concentrations of chemical species in PM_{10} and $PM_{2.5}$ during the light-firework period and the heavy-firework period.

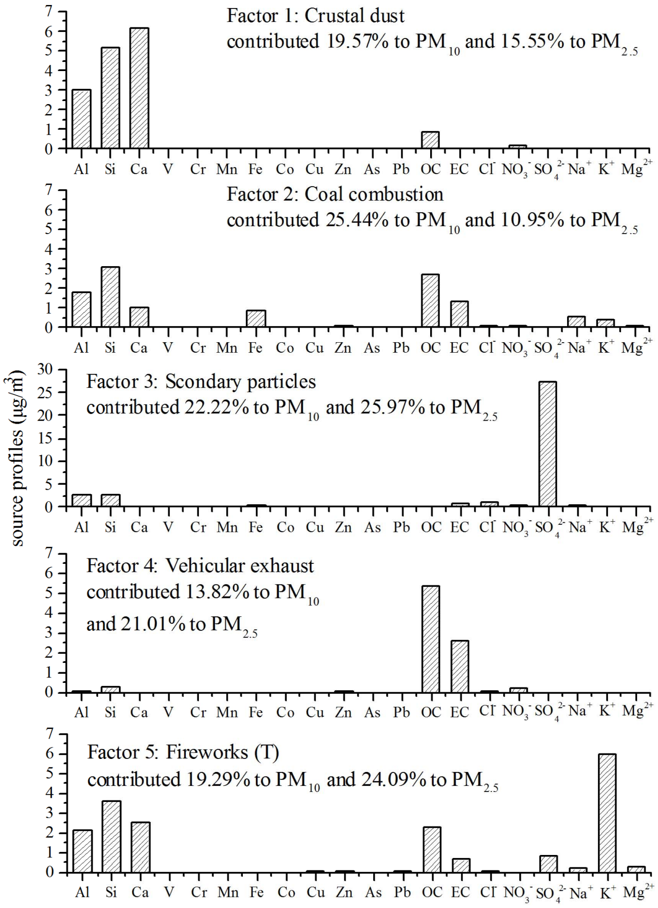

Fig. 2. Source profiles (μg m^{-3}) and percentage source contributions (%) estimated by PMF for PM$_{10}$ and PM$_{2.5}$.

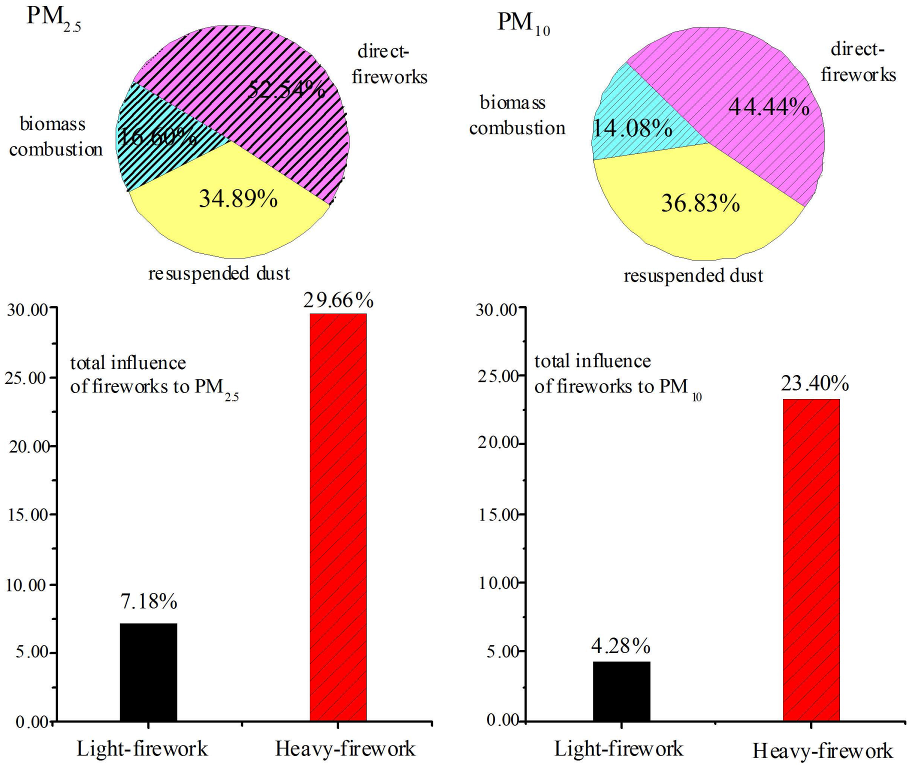

Fig. 3. The total influence of fireworks to PM_{10} and $PM_{2.5}$ (%) during the light-firework and heavy-firework periods estimated by PMF (Column chart); and individual percentage contributions to total firework impacts estimated by CMB based on Peak Analysis (Pie chart).

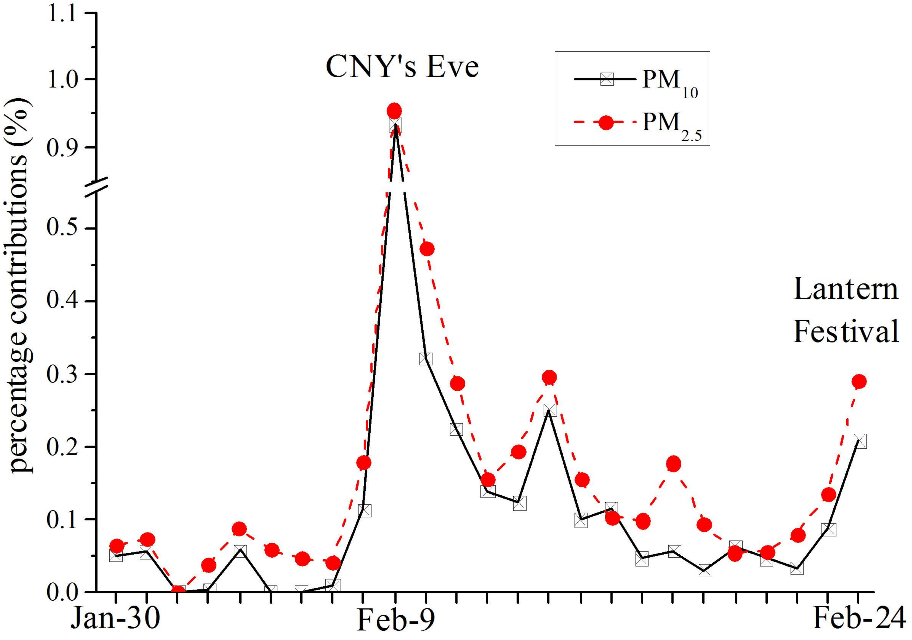

Fig. 4. The daily percentage contributions of total firework impacts to PM_{10} and $PM_{2.5}$ estimated by PMF.

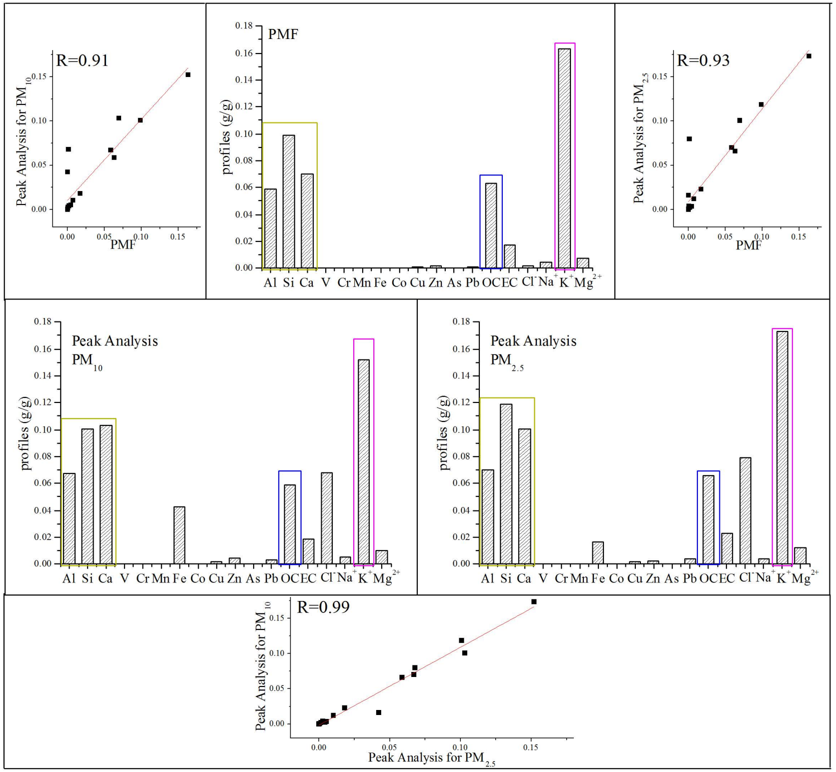

Fig. 5. Profiles of fireworks ($g\,g^{-1}$) estimated by PMF for PM_{10} and $PM_{2.5}$, Peak Analysis for PM_{10} and Peak Analysis for $PM_{2.5}$; and the regression plots between these profiles.